BMC Cancer

RESEARCH

Open Access

Anoikis-related genes in breast cancer patients: reliable biomarker of prognosis

Mingzheng Tang[1,2,3,4†], Yao Rong[2,3,4,6†], Xiaofeng Li[2†], Haibang Pan[2], Pengxian Tao[5], Zhihang Wu[2], Songhua Liu[2,3,4,6], Renmei Tang[7*], Zhilong Liu[8*] and Hui Cai[3,4,5*]

Abstract

Background Breast cancer (BC) is the most common cancer in women, and its progression is closely related to the phenomenon of anoikis. Anoikis, the specific programmed death resulting from a lack of contact between cells and the extracellular matrix, has recently been recognized as playing a critical role in tumor initiation, maintenance, and treatment. The ability of cancer cells to resist anoikis leads to cancer progression and metastatic colonization. However, the impact of anoikis on the prognosis of BC patients remains unclear.

Method This study utilized data from the Cancer Genome Atlas (TCGA) and Gene Expression Omnibus (GEO) databases to collect transcriptome and clinical data of BC patients. Anoikis-related genes (ARGs) were classified into subtypes A and B through consensus clustering. Subsequently, survival prognosis analysis, immune cell infiltration analysis, and functional enrichment analysis were performed for both subtypes. Using the Least Absolute Shrinkage and Selection Operator (LASSO) regression analysis, a set of 10 ARGs related to prognosis was identified. Immune cell infiltration and tumor microenvironment analyses were conducted on these 10 ARGs to develop a prognostic model. Furthermore, single-cell data analysis and real-time polymerase chain reaction (RT-PCR) analysis were employed to study the expression of the 10 identified prognostic ARGs in BC cells.

Results One hundred thirty-five ARGs were identified as differentially expressed genes in the TCGA and GEO databases, with 42 of them associated with the survival prognosis of BC patients. Analyses involving Principal Component Analysis (PCA), t-Distributed Stochastic Neighbor Embedding (t-SNE), and Uniform Manifold Approximation and Projection (UMAP) revealed distinct expression patterns of ARGs between types A and B. Patients in type A exhibited worse survival prognosis and lower immune cell infiltration compared to type B. Subsequent analyses identified 10 key ARGs (YAP1, PIK3R1, BAK1, PHLDA2, EDA2R, LAMB3, CD24, SLC2A1, CDC25C, and SLC39A6) relevant to BC prognosis. Kaplan–Meier analysis indicated that high-risk patients based on these ARGs had a poorer BC prognosis. Additionally, Cox regression analysis established gender, age, T (tumor), N (nodes), and risk score as predictive factors in a nomogram model for BC. The model demonstrated diagnostic value for BC patients at 1, 3, and 5 years. Decision curve analysis (DCA) verified the risk score as a reliable predictor of BC patient survival rates. Moreover, RT-PCR

†Mingzheng Tang, Yao Rong and Xiaofeng Li contributed equally to this work and share first authorship.

*Correspondence:
Renmei Tang
15008025506@163.com
Zhilong Liu
378438195@qq.com
Hui Cai
caialonteam@163.com
Full list of author information is available at the end of the article

results confirmed differential expressions of YAP1, PIK3R1, BAK1, PHLDA2, CD24, SLC2A1, and CDC25C in BC cells, with SLC39A6, EDA2R, and LAMB3 showing low expression levels.

Conclusion ARGs markers can be used as BC biomarkers for risk stratification and survival prediction in BC patients. Besides, ARGs can be used as stratification factors for individualized and precise treatment of BC patients.

Keywords Breast cancer, Anoikis, Immunity, Prognosis

Introduction

Breast cancer (BC) is the most common type of cancer in women, and it is also one of the diseases that pose a serious threat to women's health worldwide [1–3]. According to recent statistics, the incidence of BC has shown an increasing trend. According to the 2022 Global Cancer Statistics report, among all types of cancer, female breast cancer has reached the second place in the proportion of diagnosed cancers (11.6%) and the third place in deaths caused by cancer (6.9%) [4]. Although a standard multidisciplinary comprehensive treatment scheme has been formed for the treatment of breast cancer [5], including surgery, chemotherapy, endocrine therapy, targeted therapy and radiotherapy, most patients with early breast cancer can obtain a relatively good prognosis, but there are still some patients with tumor recurrence and metastasis [6]. Especially for patients with advanced breast cancer or patients with special pathological types, such as triple negative breast cancer and HER-2 positive breast cancer, the existing treatment methods are often difficult to effectively curb the progress of the disease [7]. In addition, breast cancer patients with distant metastasis usually have a poor prognosis and are prone to drug resistance, further increasing the risk of tumor recurrence [8]. Therefore, early identification and verification of reliable or more accurate biomarkers to achieve effective prediction and treatment of breast cancer is still a major challenge [9, 10].

Cell death plays a crucial role in the organism by promoting tissue development and differentiation, removing harmful or damaged cells, and maintaining homeostasis [11]. Anoikis is a specific form of programmed cell death that is triggered when cells lose interaction with the adjacent extracellular matrix (ECM) or fail to adhere to proper positions [12]. This unique mode of cell death is considered to be a physiological process closely related to body homeostasis [13]. Anoikis resistance, namely the release or avoidance of anoikis, prolongs the anchorage-independent survival time of cells, thereby promoting cell reset and uncontrolled proliferation in other sites [14, 15]. With the deepening of research, more and more evidence show that tumor cells can resist anoikis in a variety of ways, and invasive tumor cells with anoikis resistance characteristics play an important role in cancer development [16]. Resistance of cancer cells to anoikis, a phenomenon that promotes the occurrence of distant organ metastasis of cancer [17]. Moreover, studies have shown that anoikis resistance is closely related to tumor microenvironment [18], epithelial-mesenchymal transition [19] and oxidative stress [20]. These findings laid the foundation for further studies on the role of anoikis in the immune microenvironment, its impact on high—and low-risk populations, and its potential therapeutic implications (immunotherapy). VEGF secreted by endothelial cell secretory factors associated with tumor microenvironment can resist anoikis by activating PI3K/AKT [21]. EMT can make cells produce markers of anoikis resistance to phenotypic transformation [13]. Increasing the expression of EMT marker (N-cadherin) and enhancing cell migration through the activation of Polo-like kinase 4, epidermal growth factor receptor (EGFR) and Akt pathways can resist anoikis [22, 23]. The production of reactive oxygen species (ROS) by tumor cells is an indicator of oxidative stress [24]. Studies have reported that low ROS content and expression of hypoxia-inducible factors are observed in cancer cells growing in suspension [25], and upregulation of NOX4 leads to ROS production and induces anoikis resistance through the EGFR signaling pathway [26]. As an important part of the body's defense mechanism, anoikis plays an important role in maintaining body homeostasis by preventing exfoliated cells from entering unsuitable areas and inhibiting their growth [27, 28]. However, the research on the relationship between anoikis and BC is still insufficient, and there is a lack of BC risk score prediction models based on anoikis related genes (ARGs) to comprehensively reflect the impact of ARGs on the prognosis of BC patients.

At present, although the relationship between anoikis and tumors has been extensively studied, there is still a significant shortage in the study of constructing a prognostic model of ARGs in BC. In this context, our study used Cancer Genome Atlas (TCGA) and Gene Expression Omnibus (GEO) database resources to deeply explore the differential expression of ARGs in BC. Subsequently, we performed a comprehensive and systematic analysis of the differentially expressed ARGs, including LASSO regression analysis, Cox regression analysis, prognostic analysis, consensus cluster analysis, immune cell infiltration, tumor microenvironment (TME), and GO and KEGG functional enrichment analysis. Ten

ARGs closely related to prognosis were screened to construct a prognostic model. Finally, single-cell data analysis and real-time fluorescence quantitative polymerase chain reaction (RT-PCR) analysis were used to further verify the prognostic value of these ARGs in BC patients. Through the comprehensive analysis of these ARGs data, we aim to explore the practicability of ARGs in predicting the prognosis of BC patients, to provide new ideas and perspectives for new potential treatment strategies, clinical dose selection and anti-tumor targets discovery of BC, to optimize treatment options.

Materials and methods

Data collection and acquisition of anoikis genes

TCGA database (https://portal.gdc.cancer.gov) is a comprehensive resource platform, it provides the detailed clinical data of 33 kinds of malignant tumor and transcriptome RNA sequence data. These data resources are open to the public for researchers to collect and download for more detailed data analysis. Based on this platform, we successfully downloaded the transcriptome data and clinical data of BC. To further process these data, we applied Perl scripts to precisely extract and integrate the transcriptomics matrix of each BC sample, which laid a solid data foundation for the subsequent analysis work. In order to obtain the relevant information of BC patients, we conducted a comprehensive keyword search in the GEO database of NCBI (Home—GEO—NCBI (nih.gov)), using "breast cancer survival" as the key word, in order to obtain more comprehensive patient information. We respectively from GeneCard Database (GeneCards—Human Genes | Gene Database | Gene Search) [29] and Harmonizome Database (https://maayanlab.cloud/Hharmonome/) to download the ARGs genome data, and set a strict standard, The correlation coefficient > 0.4, | log2FC | > 1.0 and false discovery rate (FDR) < 0.05, in order to ensure the veracity and reliability of the data. In the process of processing these data, we used R packages "limma" and "sva" for normalization, aiming to eliminate the batch effect of the data in these four databases and further improve the accuracy and reliability of the data.

Consensus clustering

Consensus clustering is a widely used technique for cancer subtype classification. The samples can be divided into several subtypes according to different omics datasets, and then the in-depth comparative analysis of each subtype can be carried out. In this study, we performed Consensus clustering of samples based on ARGs expression using the "Consensus ClusterPlus" R package to obtain different subtype classifications. To ensure the reliability of the clustering results, we also used principal component analysis (PCA), t-distributed random neighbor embedding (t-SNE), and unified manifold approximation and projection (UMAP) to verify the consensus clustering results.

Functional enrichment analysis

Gene set variation analysis (GSVA) is an unsupervised method for estimating changes in pathway activity of samples, which is often used for data analysis of gene expression profiles [30]. To explore the biological functions of ARGs, the predefined R sets "c5.go.symbols.gmt" and "c2.cp.kegg.symbols.gmt" were used for GSVA analysis of ARGs. GO is a bioinformatics tool for annotating genes and analyzing their biological processes, covering molecular function (MF), cellular component (CC), and biological process (BP). KEGG is a database resource for understanding advanced functions and biological systems in large-scale molecular data sets generated by high-throughput experimental techniques. Subsequently, Gene Ontology (GO) and Kyoto Encyclopedia of Genes and Genomes (KEGG) enrichment analysis were performed using the "clusterProfiler"R language package to search for significantly enriched biological functions and pathways.

Characterization of ARGs development and validation

The least absolute shrinkage and selection operator (LASSO) algorithm was applied to screen the feature genes, and the best penalized regularization parameter was determined by tenfold cross-validation. Genes with relative association > 0.25 were selected as new feature genes. To eliminate the batch effect of TCGA data, we used the R package "sva" to construct the exact model. Next, we utilized the R package "glmnet" to further reduce the number of genes in the final risk score model, selecting variables with $p = 0.01$ for LASSO regression analysis. Based on the best combination of regression coefficients and λ values, we selected 10 ARGs to construct the risk scoring model. The risk score was calculated using the formula: risk score = $\sum$ (ð × Exp), where the correlation coefficients can be found in Supplementary Table S1. We randomly divided all samples into test and training groups and used the median ARGs risk score as the threshold to classify BC patients into high-risk and low-risk groups. To validate the accuracy and prognostic value of the risk scoring model, Receiver Operating Characteristic (ROC) curves, area under the curve (AUC) and Kaplan–Meier (K-M) survival curves were plotted using R software, suriminer and ggrisk software.

Characterization of ARGS and tumor microenvironment

The tumor microenvironment (TME) plays a crucial role in the pathogenesis of BC and the effect of immunotherapy. To further evaluate the correlation between

ARGs and cancer immunity, the proportion of immune cell types was estimated for the BC population in the high-risk and low-risk groups. The relative proportions of immune cells in the high-risk and low-risk populations were measured using the "CIBERSORT" and "ssGSEA" R software packages, and the sum of the total scores of all estimated immune cell types in each sample was equal to one. R packages "estimate" and "limma" were used to calculate the stromal/immune scores of BC samples simultaneously. At the same time, correlation analysis was used to explore the relationship between risk score values and immune cell infiltration. We hope to provide more accurate and effective strategies for cancer immunotherapy in the future.

Establishment of a prognostic nomogram for BC patients

By constructing a nomogram, the survival rate of BC patients can be more accurately predicted. Firstly, a nomogram model was constructed by combining the risk score with key clinical information, such as age, gender and disease stage. Calibration curves were used to verify the reliability of the nomogram. The accuracy and predictive power of the model were evaluated by comparing the overall survival (OS) of actual patients with the OS predicted by the model. To further explore whether the nomogram could be used as an independent factor to predict the prognosis of BC patients, we also performed an independent prognostic analysis. The ROC curve is a commonly used tool to evaluate the performance of prediction models. The ability of the nomogram to diagnose BC was evaluated by drawing the ROC curve and analyzing its area under the curve. Finally, decision curve analysis (DCA) was used to further validate the accuracy of the nomogram.

Tumor immunology single cell center database

Currently, a large single-cell RNA sequencing database of TME exists, called the Tumor Immune Single-Cell Center (TISCH: TISCH (comp-genomics.org)) [31]. The database is dedicated to performing rigorous data-quality checks, eliminating batch effects, clustering cells, annotating cell types, classifying malignant cells, and performing differential expression analyses. Using this database, we can perform precise and efficient analysis of prognostic signature ARGs in multiple cell types.

Cell culture

Human normal breast cells (MCF-10A) and human breast cancer cells (MDA-MB-231, T-47D, and MCF-7) purchased from the Cell Resource Center of the Chinese Academy of Sciences were deposited in the Central Laboratory of General Surgery, Gansu Provincial People's Hospital. The breast cancer cell line T-47D was cultured in RPMI-1640 medium containing 10% fetal bovine serum (FBS) and 1% double antibody (streptomycin and penicillin). Normal breast cell line MCF-10A, and breast cancer cell lines MCF7 and MDA-MB-231 were cultured in DMEM medium containing 10%FBS and 1% double antibody. All cells were placed in a dedicated incubator with 5% CO2, a constant temperature of 37° C, and appropriate humidity to ensure cell growth and reproduction under optimal conditions.

Real-time polymerase chain reaction(RT-PCR)

Total RNA was obtained from normal breast cells (MCF-10A) and BC cells (MDA-MB-231) according to the instructions of the M5 Universal RNA Mini Kit. absorbance values at 260 nm and 280 nm were determined by spectrophotometry to ensure consistent RNA concentration and purity. RNA was reverse transcribed into cDNA by quantitative PCR according to the instructions of the M5 Sprint RT kits with gDNA remover reverse transcription kits cDNA was used as template for quantitative RT-PCR detection with 2×M5 Advanced SYBR premixed EsTaq (with Tli Rna seH). ICOS primers were designed and synthesized by Bioen gineering (Shanghai) Co. All primers were designed and synthesized by Bioengineering (Shanghai) Co. The sequences of the primers are displayed in Supplementary Table S2.

Statistical analysis

All gene data in this study were log transformed to achieve normalization. Spearman's rank correlation coefficient was used to explore the correlation between ARGs expression and immune cell infiltration abundance and gene co-expression analysis. All analyses were performed with the use of R software (version 4.3.1, www.R-project.org), and the results were visualized with the use of the corresponding R packages. Graphpad Prism 8.0 software was used to analyze the RT-PCR data of this study. Measurement data were analyzed by "mean ± standard deviation" method. t test was used to analyze the data between the two groups. One-way analysis of variance was used to compare the data between multiple groups. A P value of less than 0.05 was considered to indicate statistical significance.

Results

ARGs acquisition

After a comprehensive search of Genecards and Harmonozome databases, we obtained a total of 640 ARGs (Supplementary Table 3). By integrating the information from TCGA-BC and from the GEO dataset GSE25066, we further screened 135 differentially expressed genes from the 640 ARGs (Fig. 1A and B).

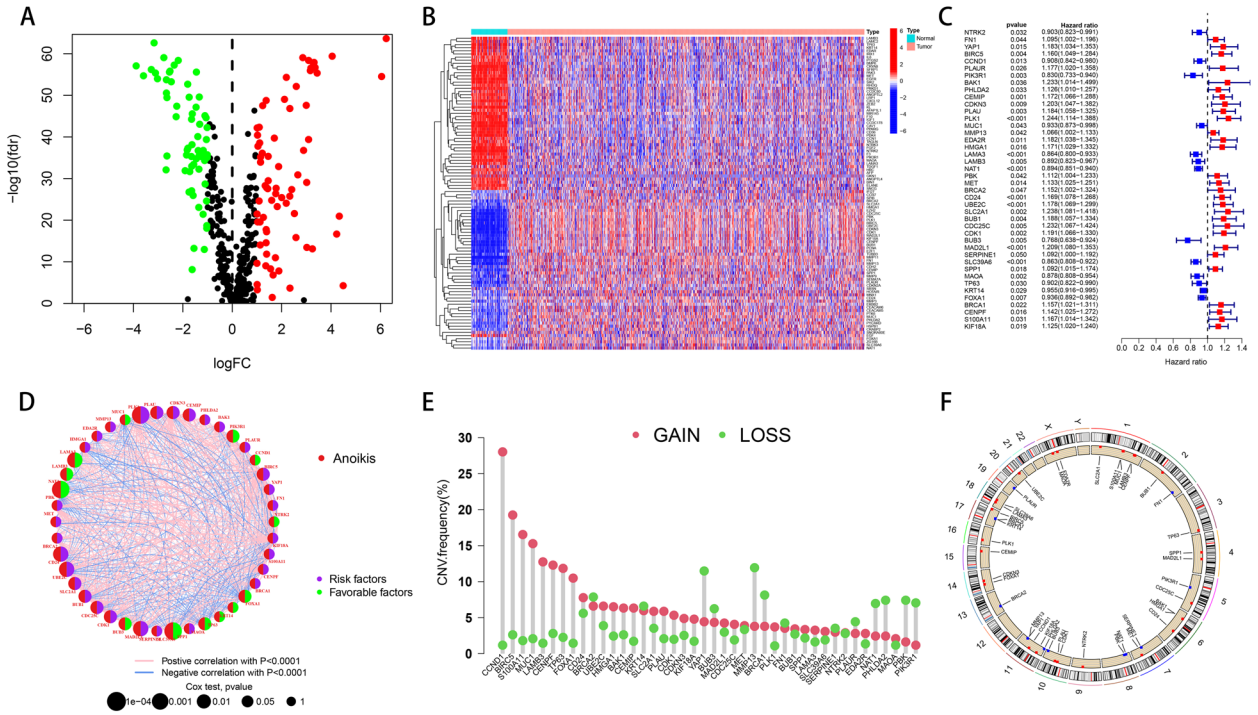

Fig. 1 Characteristics of ARGs in BC. **A** Volcano plot of 135 ARGs differentially expressed, with up-regulated genes in red and down-regulated genes in green. **B** Heat map of differential expression of 135 ARGs, blue is low expression and red is high expression. **C** Forest plots of 42 ARGs univariate Cox regression analysis. **D** Network diagram of correlations among 42 ARGs. **E** Copy number variation frequency plot of 42 ARGs. **F** Circle diagram of 42 ARGs localization in chromosomal regions

Subsequently, using univariate Cox regression analysis, we found that 42 genes of these 135 differentially expressed ARGs were significantly associated with the survival prognosis of BC patients with $p < 0.05$ (Fig. 1C). In addition, a network map was constructed to reveal the co-expression relationship among these 42 ARGs. The results showed that 12 ARGs, PIK3RI, CCND1, NTRK2, FOXA1, KRT14, TP63, SPP1, BUB3, NAT1, LAMB3, LAMA3 and MUC1, were beneficial to the prognosis of BC patients, while the remaining 30 genes were associated with poor prognosis of BC patients (Fig. 1D). To further investigate the changes of ARGs on chromosomes and the locus information of each gene on chromosomes, we downloaded the CNV data from TCGA database. Twenty-seven genes, including CCND1, BIRC5, S100A11, MUC1, LAMB3, CENPF and TP63, had higher copy number gain frequency than deletion frequency by frequency map analysis. In contrast, 13 genes, including BC2, KRT14, YAP1, and BUB3, showed a higher frequency of copy number deletions than gains (Fig. 1E). Circle plots further revealed associations between MMP13, a "loss" gene located on chromosome 11, and YAP1, as well as between CCND1 and KIF18A, a "gain" gene (Fig. 1F).

Consensus clustering of ARGs

After Consensus Cluster analysis of ARGs using the "Consensus Cluster Plus" R package, two valid subtypes, type A and type B, were obtained (Fig. 2A). In-depth analysis of the survival prognosis of these two subtypes revealed A significant prognostic difference ($p < 0.001$), in which the survival of patients with type A was significantly worse than that of patients with type B (Fig. 2B). To further verify the accuracy of consensus clustering, we used dimensionality reduction techniques such as PCA, tSNE, and UMAP. The results showed that typing A and B could indeed be effectively distinguished based on the expression levels of ARGs (Fig. 2C). In addition to focusing on the overall distribution of the 42 ARGs, we also explored in depth the differences in functional enrichment between subtypes A and B. By GSVA analysis, we performed GO and KEGG enrichment analysis of these two isoforms. GO enrichment analysis showed that it was mainly related to histone kinase activity, DNA replication, ribonucleoside metabolism, recovery of a variety of small molecular compounds, protein, and cytochrome. KEGG enrichment analysis showed that endocytosis, cell cycle, DNA replication, pentose phosphate pathway, P53 signaling pathway and NOD-like receptor signaling pathway were mainly involved (Fig. 2D).

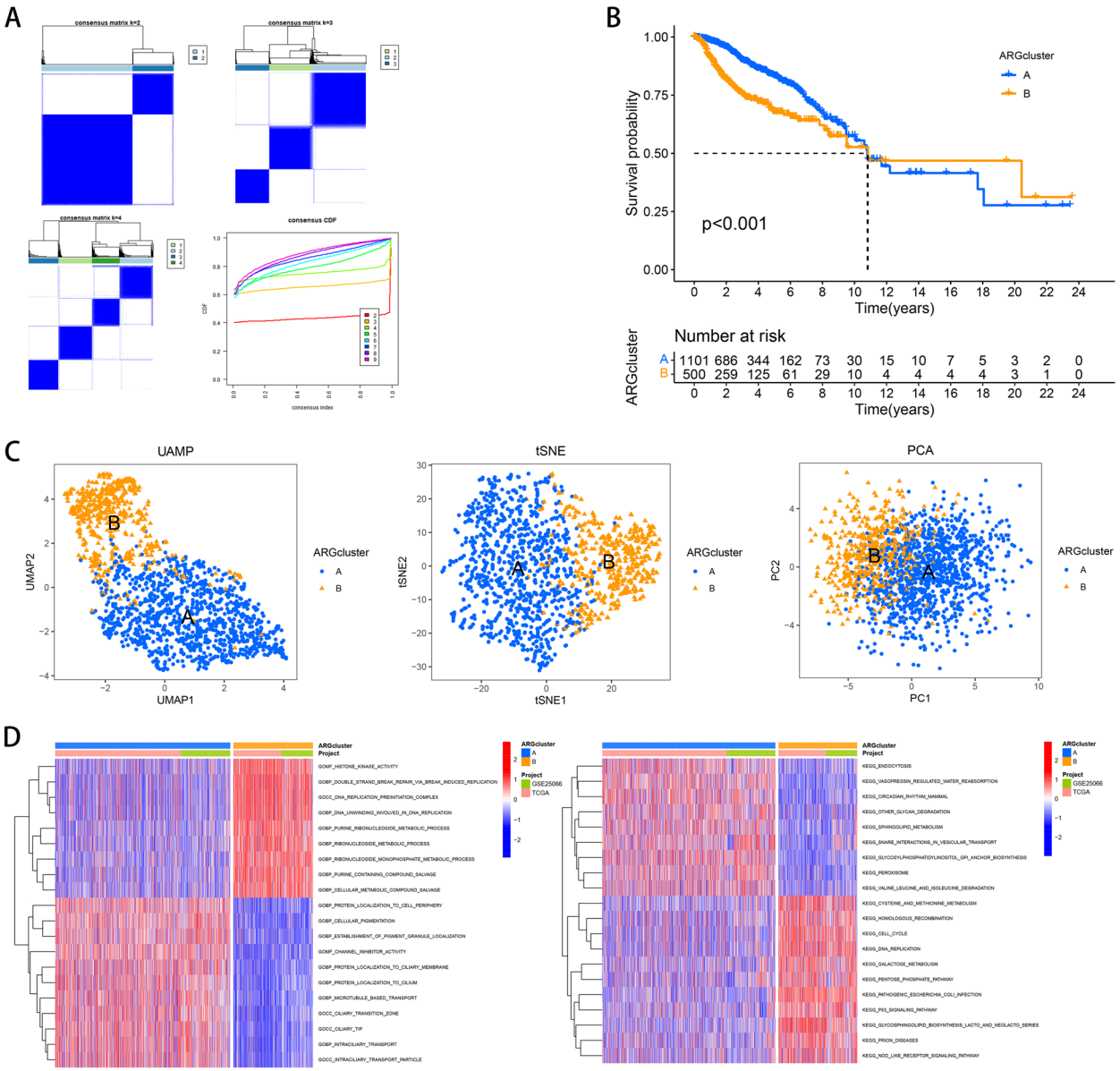

Fig. 2 ARGs Consensus clustering Characteristics. **A** Typing A and typing B were selected by consensus clustering; Consensus clustering method was used to screen out type A and type B. Color chart represents the samples can be divided into 2, 3, 4, 5, 7, 7, 8, 9 subtypes of related trends, the sample is divided into A and B two subtypes results more reliable. **B** overall survival of type A and type B. **C** In sequence, UAMP, tSNE, and PCA methods distinguish types A and B according to the expression of ARGs. **D** GSVA analysis of differential enrichment analysis of GO and KEGG between types A and B

Immune infiltration and differential gene analysis of subtyping A and B

By immune cell infiltration analysis, it was found that the level of immune cell infiltration was significantly different between type A and type B, and the percentage of immune cell infiltration in type A was lower than that in type B. Of note, CD56 natural killer cells, mast cells, neutrophils, and eosinophils were predominantly expressed in type A, whereas activated B cells, CD4-activated T cells, CD8-activated T cells, and monocytes were predominantly expressed in type B (Fig. 3A).

To further explore the expression of ARGs in subtyping A and B, we performed differential analysis. The results showed that BUB3, CCND1, SLC39A6, NAT1 and FOXA1 were up regulated in subtype A. In contrast, in subtype B, the expression of CD24, CDC25C, BUB1, PBK, CDK1, and MAD2L1 was upregulated (Fig. 3B and C). Functional enrichment analysis of these differentially

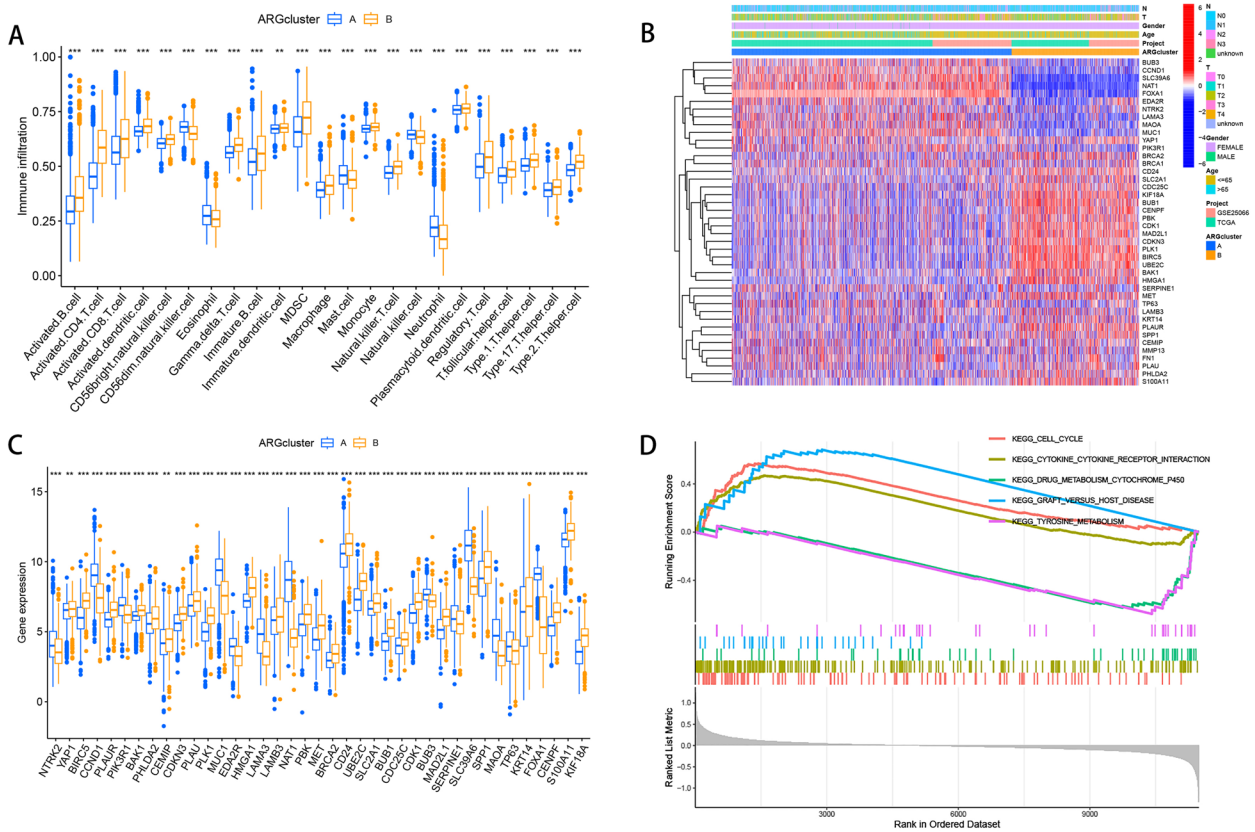

Fig. 3 Immune infiltration and differential gene analysis between types A and B. **A** Levels of immune infiltration in subtyping A and B. **B** Heat map of differential ARGs expression between subtyping A and B. **C** Box plot of differential ARGs expression between subtyping A and B. **D** enrichment analysis; Graph peaks at the top left indicate that these pathways are active, and peaks at the bottom right indicate that the pathways are silent. **P* < 0.05, ***P* < 0.01, ****P* < 0.001

expressed genes revealed that these genes were closely related to biological processes such as "channel inhibitor activity", "cell cycle", and "transplantation versus host disease" (Fig. 3D).

ARGs determination and validation

We performed LASSO regression analysis using 42 ARGs that were strongly associated with the prognosis of BC patients (Fig. 4A and B). The results showed that 10 ARGs could be used as independent prognostic genes for BC patients. Among them, CD24, PHLDA2, SLC2A1, YAP1, CDC25C, and EDA2R were identified as high-risk genes, while SLC39A6, LAMB3, BAK1, and PIK3R1 were identified as low-risk genes (Fig. 4C). To further validate the prognostic impact of these genes, we explored the TCGA-BC cohort in depth using K-M survival analysis. The results showed that the prognosis of BC patients in the high-risk group was significantly worse (Fig. 4D). In addition, the complex relationships among ARGs, types A and B, risk scores, and survival status are clearly shown in Sankey plots (Fig. 4E). As shown in Fig. 4F, there was A significant difference in risk scores between type A and type B ($p < 0.05$). TCGA database was used to understand the expression of these 10 ARGs in BC, and the results showed that except for four genes (YAP1, EDA2R, LAMB3 and PIK3R1), the remaining six genes were highly expressed in BC (Fig. 4G).

Immune infiltration in different risk groups

The risk scores of BC samples are arranged in ascending order to illustrate the alterations in the proportions of diverse immune cells (Fig. 5A). The proportions of activated CD4 memory T cells, activated dendritic cells, follicular helper T cells, M0 macrophages, activated mast cells, neutrophils, and resting NK cells increased progressively with increasing risk scores (Fig. 5B). M0 macrophages were highly expressed in the high-risk group (Fig. 5C). The 10 genes that were used to construct the risk score also have strong connections with many immune cells (Fig. 5D). In addition, the Stromal score and immune score of the high-risk and low-risk groups

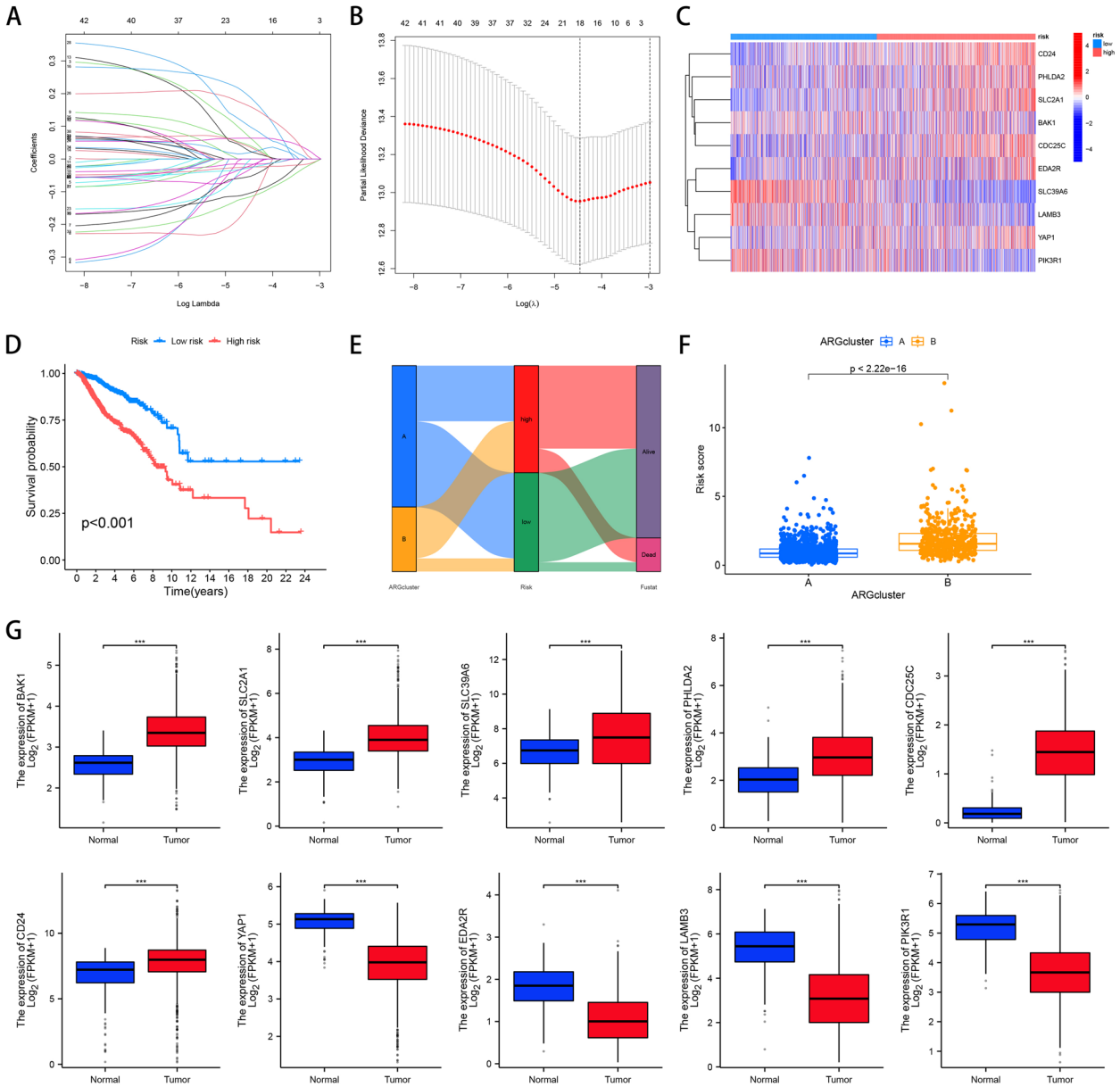

Fig. 4 Characteristics of independent prognostic ARGs. **A** Ten prognostic genes were identified by LASSO regression analysis and tenfold cross validation; Each curve corresponds to one gene. **B** coefficient distribution map of 10 prognostic genes; Vertical dashed lines are drawn at the optimal λ. **C** Risk heat map of 10 prognostic genes, red for high risk and blue for low risk (**D)** KM curves show prognosis of BC patients in high and low risk groups. **E** Sangproduct plots of the relationships between ARGs, subtypes A and B, risk scores, and survival status. **F** expression of subtypes A and B in risk scores. **G** Expression of YAP1, CD24, SLC39A6, CDC25C, BAK1, EDA2R, LAMB3, PHLDA2, PIK3R1 and SLC2A1 in BC in TCGA database

were determined from the estimated value of the expression profile (Fig. 5E).

Establishment of a prognostic Nomogram for BC patients

After Cox multivariate regression analysis with p values significantly less than 0.05, we confirmed that gender, age, T1, T2, N1, N2, and risk score were independent predictors of BC in the TCGA cohort (Fig. 6A). Subsequently, we constructed a nomogram based on the key information of gender, age, T (tumor), N (nodes) and risk score (Fig. 6B). To verify the accuracy of the prediction model, calibration curves were drawn to compare the agreement between the overall survival (OS) predicted by the model and the actual OS at 1, 3, and 5 years for

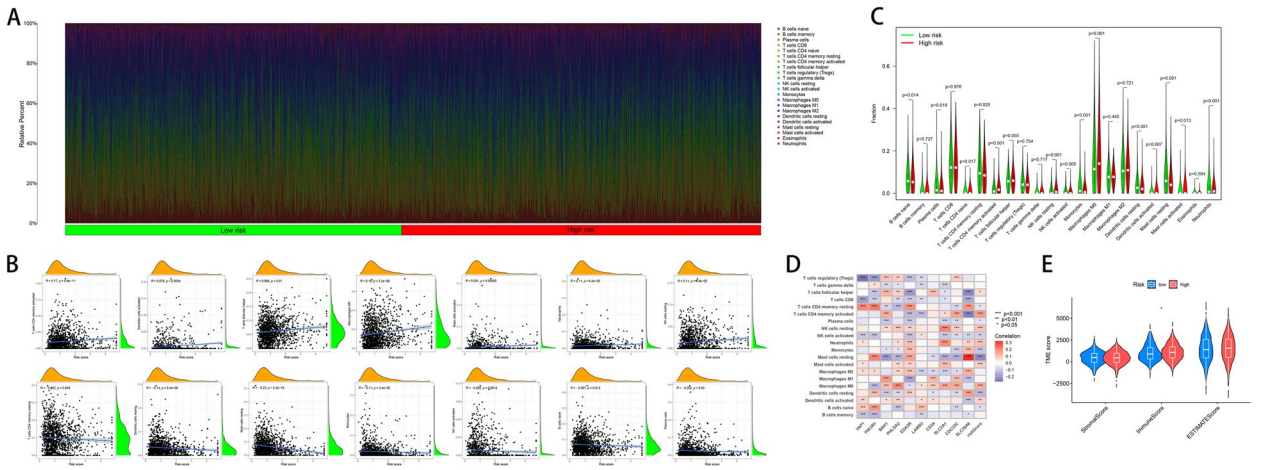

Fig. 5 Tumor immune microenvironment with different risk scores. **A** Relative proportions of high-risk versus low-risk immune cell infiltration. **B** Correlation analysis between risk score and proportion of each cell. **C** differences in immune cell composition between high-risk and low-risk populations. **D** Correlation between immune cells and 10 prognostic ARGs. **E** Stromal score and Immune score of high-risk group and low-risk group. $^{*}P < 0.05$, $^{**}P < 0.01$, $^{***}P < 0.001$

BC patients. The results showed that the predicted OS of the nomogram was close to the actual OS, indicating that the model could accurately predict the OS of BC patients (Fig. 6C). Furthermore, time-dependent ROC curves were plotted to evaluate the predictive performance of the model. In the TCGA cohort, this prognostic model showed above-average diagnostic value for BC patients at 1, 3, and 5 years (Fig. 6D). Finally, we analyzed the performance of the risk score in predicting BC patients using DCA curves. The results showed that the risk score was a good predictor over time horizons of 1, 3, and 5 years (Fig. 6E).

Correlation analysis of ARGS and TME

We downloaded the single-cell dataset EMTAB8107 of BC through the TISCH database (http://tisch.compgenomics.org/) and then examined the expression of 10 ARGS in TME. The EMTAB8107 dataset contains 19 cell populations and 11 intermediate cell types, and the photos show their distribution and numbers (Fig. 7A.). CD24 and SLC39A were mainly expressed in malignant cells. PHLDA2 and YAP1 were mainly expressed in myofibroblast cells. In contrast, PIK3R1 and BAK1 were more uniformly expressed in individual cells (Fig. 7B and C).

RT-PCR validation of prognosis-related ARGS

To further explore the expression of ARGs related to prognosis, we selected normal cell line (MCF-10A) and breast cancer cell lines (MDA-MB-231, T-47D and MCF-7) as experimental subjects to verify the expression levels of 10 specific genes. By RT-PCR analysis, we found that the expression levels of seven ARGs, YAP1, PIK3R1, BAK1, PHLDA2, CD24, SLC2A1 and CDC25C, were significantly increased in breast cancer cells. However, the expression of three ARGs, SLC39A6, EDA2R and LAMB, was significantly reduced in breast cancer cells (Fig. 8). These results suggest that these genes may be closely related to the prognosis of breast cancer and may be used as key biomarkers for the prognosis evaluation of breast cancer.

Discussion

In the absence of extracellular matrix attachment, the integrin attachment of cells is disrupted, which in turn triggers anoikis, a type of programmed cell death [32, 33]. Anoikis helps to prevent the deposition of isolated epithelial cells at other sites and is important for tissue homeostasis and development [32]. Dysregulated anoikis has become characteristic of cancer cells and drives metastasis to distant organs [34]. However, the relationship between anoikis and BC remains unclear.

This study, based on the TCGA-BC project, identified specific ARGs in BC. Then, all patients were divided into training and testing cohorts. By multivariate Cox regression analysis, ten ARGs related to prognosis were screened out, and a risk score prognostic model was constructed. To ensure the performance of the ARGs model, we constructed an ARGs based nomogram, which included age, T (tumor), N (nodes), and risk score. The calibration plot showed that the model had a high fit in predicting prognosis. Seven ARGs were upregulated in BC cells, including YAP1, PIK3R1, BAK1, PHLDA2, CD24, SLC2A1 and CDC25C. The expression levels of EDA2R, LAMB3 and SLC39A6 were decreased.

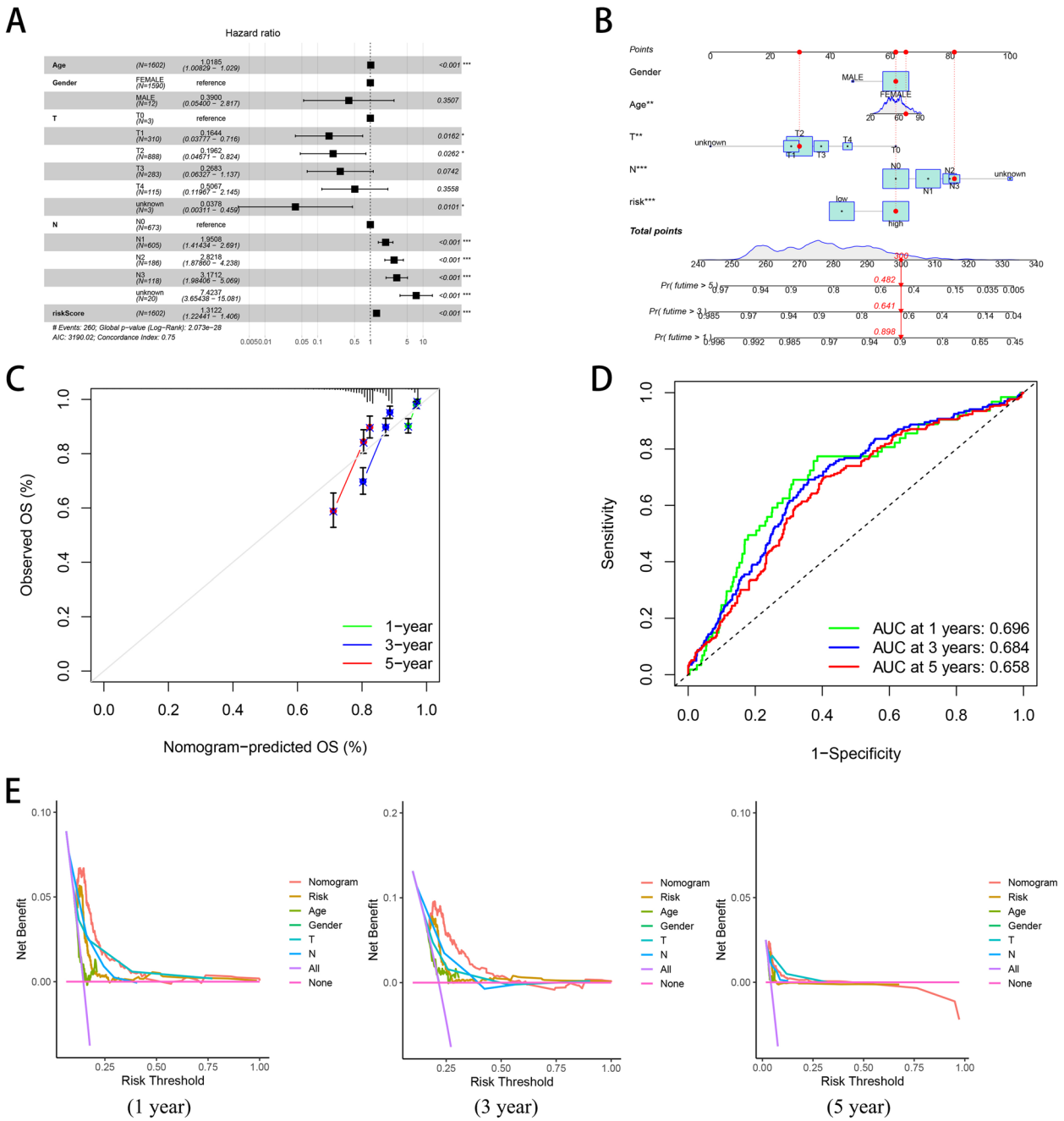

Fig. 6 Features for constructing prognostic models. **A** TCGA cohort multivariate COX analysis to assess risk scores and clinical characteristics (including age, grade, sex). **B** Nomograms for risk scores and clinical characteristics predicting survival at 1, 3, and 5 years. **C** Calibration curve. **D** ROC curve. **E** DCA curves for risk scores and clinical characteristics *$p < 0.05$, ***$p < 0.001$

In recent years, many studies have been devoted to the construction of prognostic models of ARGs in cancer. However, compared with previous studies, 640 ARGs were included in this study. In contrast, the previous study only selected 434 ARGs through GeneCards database and did not involve ARGs in Harmonozome database [35]. Of note, although studies have explored the role of ARGs in non-cancer diseases, they are relatively few, and no prognostic models have been constructed or PCR-based cell experiments have been performed to verify ARGs expression [36]. In addition, there are still studies on the prognostic significance of anoikis-related lncRNAs, immune microenvironment characteristics, ceRNA regulatory network and traditional Chinese

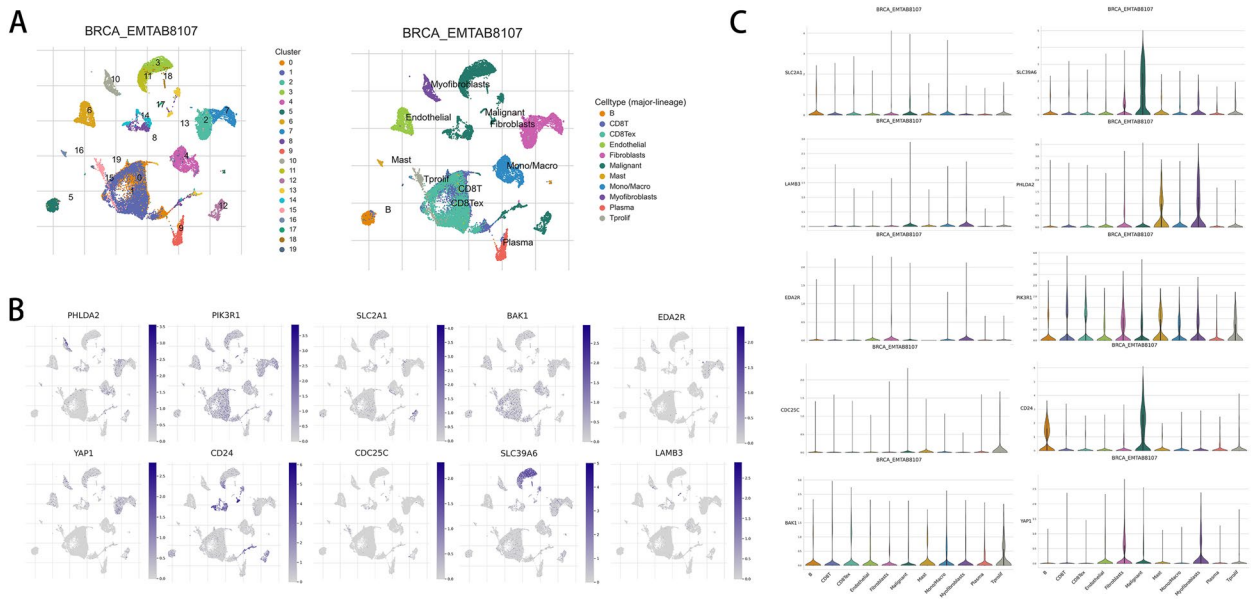

Fig. 7 Ten ARGs in single-cell RNA sequencing. **A** EMTAB8107 for all cell types in single-cell RNA sequencing and percentages for each cell type. **B**, **C** Expression of YAP1, CD24, SLC39A6, CDC25C, BAK1, EDA2R, LAMB3, PHLDA2, PIK3R1, and SLC2A1 in each cell type

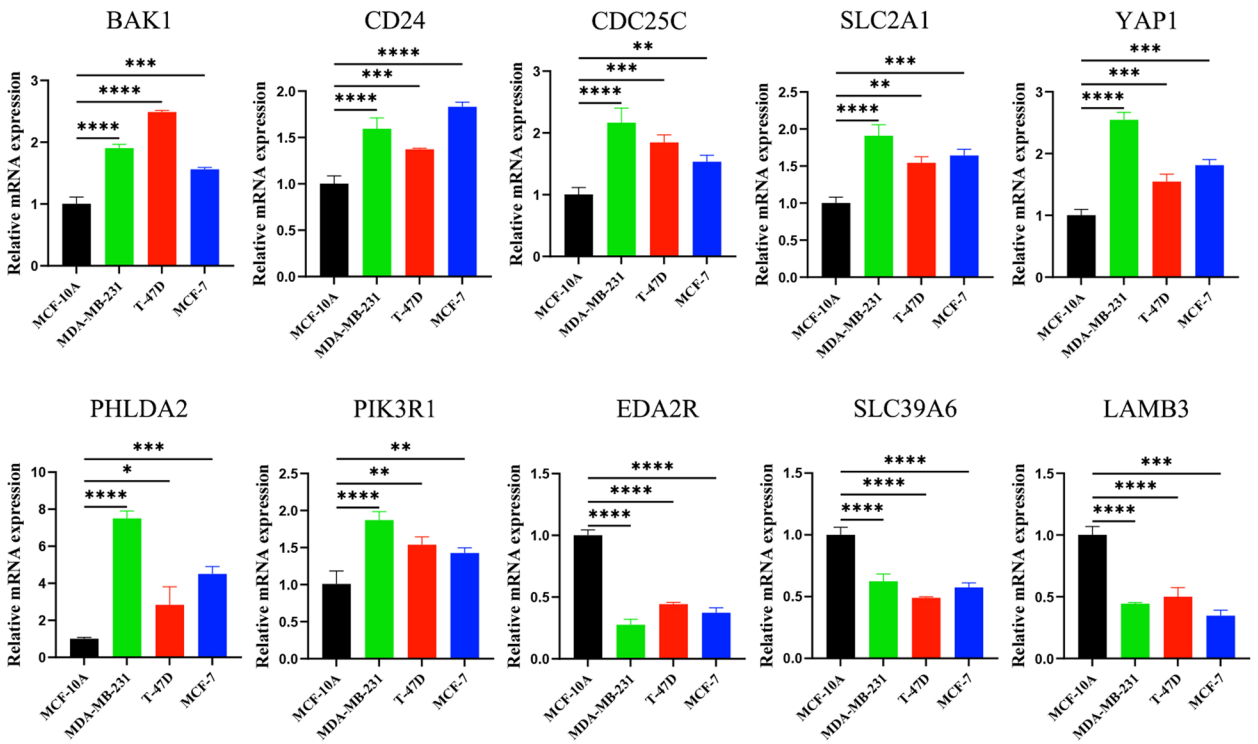

Fig. 8 RT-PCR analysis of ARGs. The normal cell line was MCF-10A, and the BC cell lines were MDA-MB-231, T-47D, and MCF-7. *$P < 0.05$, **$P < 0.01$, ***$P < 0.001$, ****$P < 0.0001$

medicine [37, 38]. Although the existing literature has emphasized the relationship between ARGs and diseases, there are still many unknowns to be revealed. Future studies may consider exploring how anoikis affects disease-related mechanisms to improve patient treatment and overall survival.

To explore the functions of ARGs, in this research, GO and KEGG functional enrichment analyses were performed on ARGs. GO enrichment analysis showed that ARGs were mainly related to histone, protein, cytochrome and ribonucleoside metabolism. Existing studies have shown that chlordane diterpenoids, a class of bicyclic diterpenoids widely present in hundreds of plant species, can induce anoikis of bladder cancer cells by inducing histone deacetylases, thereby inhibiting their migration and invasion [39]. Anoikis resistance is mediated by two pathways related to anchor independent growth proteins and EMT [40]. Low and medium doses of cadmium exposure can up-regulate cytochrome P450 enzymes, activate nuclear receptor-mediated extrinsic detoxification pathways, and induce FAK-mediated anoikis activation in the kidney [41]. In addition, KEGG enrichment analysis results showed that ARGs were mainly related to cell cycle, pentose phosphate pathway and P53 signaling pathway. The results of this study are consistent with those of previous studies. Cyclin D1 and MAPK-mediated survival pathways, as well as inhibition of epithelial genes, can maintain the EMT phenotype in cancer cell populations, resulting in anoikis resistance [16]. P-cadherin can induce anoikis resistance in stromal exfoliated BC cells by promoting the pentose phosphate pathway and reducing oxidative stress [42]. Kim's research team [43] experimentally demonstrated that AtG5-mediated autophagy regulates anoikis of fibroblasts in nude mice through the p53 pathway. These studies confirmed the reliability of the results of the present study. Interestingly, the role of nucleotide metabolism in mediating anoikis resistance has not been fully resolved. This may be a promising approach for future research aimed at modulating nucleotides to enhance tumor metastasis [13].

The TME, or tumor microenvironment, is composed of immune cells, stromal cells, and tumor cells. TME can stimulate the heterogeneity between tumor cells and make them multidrug resistant, thereby promoting the progression and metastasis of tumor cells [44]. At the same time, TME has a major impact on the spontaneous recognition of the immune system and the mediation of malignant tumors. Studies have found that the anti-tumor effect is more significant when immune cells are located between tumor cells rather than between stromal cells [45]. The innate and adaptive immune systems jointly recognize and eliminate tumor cells, and various immune cells play different roles [46]. In this study, immune cell analysis revealed that natural killer cells, B cells, CD8-activated T cells, and monocytes were highly expressed in ARGs typing. Previous studies have shown that anoikis is associated with a variety of immune cells. For example, anoikis-resistant cells have enhanced cell motility and the ability to evade immune surveillance mediated by natural killer cells and have a significant advantage in the formation of lung metastatic lesions in mice [47]. Signals from B-cell antigen receptors and chemokine receptors play a central role in regulating the interaction of normal and malignant B cells with the microenvironment [48]. Therefore, targeted regulation of integrin-mediated retention of macroglobulinemia cells in the bone marrow to mobilize malignant cells and induce anoikis may be an effective strategy for the treatment of macroglobulinemia [48]. Polo-Generelo et al. reported [49] that the Serpine1 gene itself can confer mesenchymal properties to cells, promote migration, invasion, and anoikis resistance, and promote CD8 + T cell clearance from colon adenocarcinoma. During the differentiation of human monocytes, LDL stimulates the expression of cell adhesion molecules, down-regulates the apoptotic effector molecules of early macrophages, and regulates anoikis [50]. In addition, we explored the differences in immune microenvironment, TME score and performance of immune status between low-risk and high-risk patients. The results showed that with the increase of risk score, the proportion of activated CD4 memory T cells, activated dendritic cells, follicular helper T cells, M0 macrophages, activated mast cells, neutrophils and resting NK cells gradually increased. This suggests that anoikis may regulate BC progression by affecting the level of immune infiltration. Previous studies have found that MDR1-expressing CD4 + T cells with Th1.17 features resist to neoadjuvant chemotherapy and are associated with breast cancer clinical response [51]. Turpin's team [52] established a culture model of BC patient-derived explants and found that respiratory complex I regulates dendritic cell maturation in an explant model of human tumor immune microenvironment. Functional Th1-directed follicular helper T cells in human BC can promote effective adaptive immunity [53]. ZNF746 promotes macrophage polarization and enhances BC cell proliferation, migration, and invasion through Jagged1/Notch pathway [54]. Tumor-infiltrating immune cells (mast cells and neutrophils) can affect the response to neoadjuvant chemotherapy in BC [55]. CCL5/IFNγ-CXCL9/10 axis triggered by natural killer cells is the basis for the clinical efficacy of neoadjuvant anti-HER-2 antibody in BC [56]. These existing findings are mutually validated with the results of the present study, which enhances the credibility of the results of the present study. Therefore, in-depth study of the mechanisms of anoikis and immunity may reveal new targeted therapies for cancer treatment (immunotherapy).

The results of this study show that characteristic ARGs can accurately predict the prognosis of BC, and clinical variables with high-risk scores are often statistically significant risk factors for prognosis, suggesting that ARGs

genetic signatures can be used as prognostic indicators. Studies have shown that patients with higher risk scores tend to have higher tumor grades, suggesting a high risk of poor prognosis [57, 58]. Interestingly, ten prognostic related ARGs in this study have been widely reported in relation to BC mechanisms. YAP1 overexpression affects the prognosis of HER2-positive patients. BCAR4 promotes trastuzumab resistance and EMT in BC by spongifying miR-665 and interacting with YAP1 [59, 60]. Somatic loss of PIK3R1 may sensitify BC to MAPK pathway inhibitors [61]. Bak1 is a proapoptotic protein that can induce apoptosis of BC cells [62]. The relationship between EDA2R and BC remains unclear, but EDA2R-NIK signaling promotes muscle atrophy associated with cancer cachexia [63]. Zhu et al. [64] revealed that LAMB3 promotes tumors through AKT-FOXO3/4 axis and indicated that LAMB3 is a BC cell super enhancer. CD24 is overexpressed in a variety of cancers and cancer stem cells, and is positively correlated with the pathological grade and prognosis of cancer [65]. Moreover, CD24 may be used as an immunotherapy target for triple-negative BC by regulating PD-L1 expression [66]. SLC2A1 (also known as GLUT1) plays a key role in tumor growth, invasion, metastasis, and glucose metabolism, and is associated with adverse pathological prognostic factors in BC patients [67, 68]. Diosgenin, a natural steroidal sapogenin, induces G2/M phase arrest by activating the CDC25C regulatory pathway, thereby promoting apoptosis of human BC cells [69]. High SLC39A6 nuclear expression and mRNA levels were positively correlated with estrogen receptor-positive BC expression, and high SLC39A6 expression was independently associated with longer BC specific survival [70]. Therefore, it is necessary to explore how these 10 ARGs affect anoikis or its resistance in cancer in the future to help further develop strategies against cancer metastasis.

Although our study verified the expression of ten prognosis related ARGs in BC cells and the ability of the proposed ARGs to predict the prognosis of BC patients, there are still some limitations of this study. Firstly, the clinical data of all analyzed BC cases were derived from public databases, which lacked internal data validation. Secondly, although studies have revealed the association between ARGs and immunity, the specific mechanism is still unknown. Third, the effectiveness of prediction models based on ARGs has not been verified by large-scale clinical samples. In summary, this study urgently needs to further carry out large-sample, multi-center clinical research, cell, and animal experiments to fully reveal the important role of ARGs in BC and provide guidance for the subsequent exploration of the role of ARGs in BC. Combining the results of this analysis with the previous literature, we have reason to believe that the anoikis related markers and the potential mechanism of BC immune microenvironment are full of research prospects and worthy of further exploration in the future.

Conclusions

In conclusion, our 10 ARGS features can well predict the survival rate of BC patients, and Nomogram better helps clinicians to develop various treatment plans and provide personalized treatment for patients. In the future, we need to conduct more research on the mechanism of anokis and BC action to provide clinicians with a more solid theoretical basis and provide a way forward for precision medicine.

Supplementary Information

The online version contains supplementary material available at https://doi.org/10.1186/s12885-024-12830-5.

Supplementary Material 1.

Supplementary Material 2.

Supplementary Material 3.

Acknowledgements

We thank Yan Zhang, Guiqian Zhang and Fengyuan Dong for their suggestions for this study. We acknowledge such as TCGA and GEO database for providing their platforms and contributors for uploading their meaningful datasets.

Authors' contributions

Mingzheng Tang, Yao Rong and Xiaofeng Li conceived and designed the study. Mingzheng Tang wrote the manuscript. Renmei Tang, Zhilong Liu, and Hui Cai revised the manuscript. Haibang Pan, Pengxian Tao, Zhihang Wu and Songhua Liu performed all data collection and analysis. All authors read and approved the final manuscript.

Funding

This work was supported by grants from Natural Science Foundation of Gansu Province (No.23JRRA1756).

Availability of data and materials

The data generated and analysed during the current study are available in the TCGA website (https://portal.gdc.cancer.gov), GEO (Home—GEO—NCBI (nih.gov)), GeneCard database (GeneCards—Human Genes | Gene Database | Gene Search), TISCH: TISCH (comp-genomics.org)), and Harmonomeportals (https://maayanlab.cloud/Hharmonome/). The original contributions presented in the study are included in the article/Supplementary Material, further inquiries can be directed to the corresponding author.

Declarations

Ethics approval and consent to participate

Ethics approval and consent to participate. Databases such as TCGA and GEO are public databases. The patients involved in the database have obtained ethical approval. Users can download relevant data for free for research and publish relevant articles. Our study is based on open-source data, so there are no ethical issues and other conflicts of interest.

Consent for publication

Not applicable.

Competing interests

The authors declare no competing interests.

Author details
[1]Department of Breast and Thyroid Surgery, The Second Affiliated Hospital of Hainan Medical University, Haikou, China. [2]The First Clinical Medical College of Gansu University of Chinese Medicine, Lanzhou, China. [3]Key Laboratory of Molecular Diagnostics and Precision Medicine for Surgical Oncology in Gansu Province, Gansu Provincial Hospital, Lanzhou, China. [4]NHC Key Laboratory of Diagnosis and Therapy of Gastrointestinal Tumor, Gansu Provincial Hospital, Lanzhou, China. [5]General Surgery Clinical Medical Center, Gansu Provincial Hospital, Lanzhou, China. [6]General Surgery Department, General Hospital of Southern Theater Command, Guangzhou, China. [7]Qionghai People's Hospital Breast and Thyroid Surgery, Qionghai, China. [8]Department of Anesthesiology, Gansu Provincial Hospital, Lanzhou, China.

Received: 25 February 2023 Accepted: 20 August 2024
Published online: 19 September 2024

References

1. Wang J, Sui L, Huang J, Miao L, Nie Y, Wang K, Yang Z, Huang Q, Gong X, Nan Y, et al. MoS(2)-based nanocomposites for cancer diagnosis and therapy. Bioact Mater. 2021;6(11):4209–42.
2. Torul H, Yarali E, Eksin E, Ganguly A, Benson J, Tamer U, Papakonstantinou P, Erdem A. Paper-based electrochemical biosensors for voltammetric detection of miRNA biomarkers using reduced graphene oxide or MoS(2) nanosheets decorated with gold nanoparticle electrodes. Biosensors (Basel). 2021;11(7):236.
3. Zhu L, Zhao J, Guo Z, Liu Y, Chen H, Chen Z, He N. Applications of aptamer-bound nanomaterials in cancer therapy. Biosensors (Basel). 2021;11(9):344.
4. Bray F, Laversanne M, Sung H, Ferlay J, Siegel RL, Soerjomataram I, Jemal A. Global cancer statistics 2022: GLOBOCAN estimates of incidence and mortality worldwide for 36 cancers in 185 countries. CA Cancer J Clin. 2024;74(3):229–63.
5. Cardoso MJ, Poortmans P, Senkus E, Gentilini OD, Houssami N. Breast cancer highlights from 2023: knowledge to guide practice and future research. Breast. 2024;74:103674.
6. de Boniface J, Filtenborg Tvedskov T, Rydén L, Szulkin R, Reimer T, Kühn T, Kontos M, Gentilini OD, Olofsson Bagge R, Sund M, et al. Omitting axillary dissection in breast cancer with sentinel-node metastases. N Engl J Med. 2024;390(13):1163–75.
7. Rubin E, Shan KS, Dalal S, Vu DUD, Milillo-Naraine AM, Guaqueta D, Ergle A. Molecular targeting of the Human Epidermal Growth Factor Receptor-2 (HER2) genes across various cancers. Int J Mol Sci. 2024;25(2):1064.
8. Wong GL, Manore SG, Doheny DL, Lo HW. STAT family of transcription factors in breast cancer: pathogenesis and therapeutic opportunities and challenges. Semin Cancer Biol. 2022;86(Pt 3):84–106.
9. Akgönüllü S, Bakhshpour M, Pişkin AK, Denizli A. Microfluidic systems for cancer diagnosis and applications. Micromachines (Basel). 2021;12(11):1349.
10. Al-Tashi Q, Saad MB, Muneer A, Qureshi R, Mirjalili S, Sheshadri A, Le X, Vokes NI, Zhang J, Wu J. Machine learning models for the identification of prognostic and predictive cancer biomarkers: a systematic review. Int J Mol Sci. 2023;24(9):7781.
11. Yang S, Hu C, Chen X, Tang Y, Li J, Yang H, Yang Y, Ying B, Xiao X, Li SZ, et al. Crosstalk between metabolism and cell death in tumorigenesis. Mol Cancer. 2024;23(1):71.
12. Raeisi M, Zehtabi M, Velaei K, Fayyazpour P, Aghaei N, Mehdizadeh A. Anoikis in cancer: the role of lipid signaling. Cell Biol Int. 2022;46(11):1717–28.
13. Adeshakin FO, Adeshakin AO, Afolabi LO, Yan D, Zhang G, Wan X. Mechanisms for modulating anoikis resistance in cancer and the relevance of metabolic reprogramming. Front Oncol. 2021;11:626577.
14. Du S, Yang Z, Lu X, Yousuf S, Zhao M, Li W, Miao J, Wang X, Yu H, Zhu X, et al. Anoikis resistant gastric cancer cells promote angiogenesis and peritoneal metastasis through C/EBPβ-mediated PDGFB autocrine and paracrine signaling. Oncogene. 2021;40(38):5764–79.
15. Khan SU, Fatima K, Malik F. Understanding the cell survival mechanism of anoikis-resistant cancer cells during different steps of metastasis. Clin Exp Metastasis. 2022;39(5):715–26.
16. Sobhi Amjad Z, Shojaeian A, Sadri Nahand J, Bayat M, Taghizadieh M, Rostamian M, Babaei F, Moghoofei M. Oncoviruses: Induction of cancer development and metastasis by increasing anoikis resistance. Heliyon. 2023;9(12):e22598.
17. Yu Y, Song Y, Cheng L, Chen L, Liu B, Lu D, Li X, Li Y, Lv F, Xing Y. CircCEMIP promotes anoikis-resistance by enhancing protective autophagy in prostate cancer cells. J Exp Clin Cancer Res. 2022;41(1):188.
18. Gulia S, Chandra P, Das A. The prognosis of cancer depends on the interplay of autophagy, apoptosis, and anoikis within the tumor microenvironment. Cell Biochem Biophys. 2023;81(4):621–58.
19. Tedja R, Alvero AB, Fox A, Cardenas C, Pitruzzello M, Chehade H, Bawa T, Adzibolosu N, Gogoi R, Mor G. Generation of stable epithelial-mesenchymal hybrid cancer cells with tumorigenic potential. Cancers (Basel). 2023;15(3):684.
20. Adeshakin FO, Adeshakin AO, Liu Z, Cheng J, Zhang P, Yan D, Zhang G, Wan X. Targeting oxidative phosphorylation-proteasome activity in extracellular detached cells promotes anoikis and inhibits metastasis. Life (Basel). 2021;12(1):42.
21. Bhat AA, Yousuf P, Wani NA, Rizwan A, Chauhan SS, Siddiqi MA, Bedognetti D, El-Rifai W, Frenneaux MP, Batra SK, et al. Tumor microenvironment: an evil nexus promoting aggressive head and neck squamous cell carcinoma and avenue for targeted therapy. Signal Transduct Target Ther. 2021;6(1):12.
22. Peppicelli S, Ruzzolini J, Bianchini F, Andreucci E, Nediani C, Laurenzana A, Margheri F, Fibbi G, Calorini L. Anoikis resistance as a further trait of acidic-adapted melanoma cells. J Oncol. 2019;2019:8340926.
23. Fonseca I, Horta C, Ribeiro AS, Sousa B, Marteil G, Bettencourt-Dias M, Paredes J. Polo-like kinase 4 (Plk4) potentiates anoikis-resistance of p53KO mammary epithelial cells by inducing a hybrid EMT phenotype. Cell Death Dis. 2023;14(2):133.
24. Alfaleh MA, RazeethShait Mohammed M, Hashem AM, Abujamel TS, Alhakamy NA, Imran Khan M. Extracellular matrix detached cancer cells resist oxidative stress by increasing histone demethylase KDM6 activity. Saudi J Biol Sci. 2024;31(1):103871.
25. Maurer GD, Brucker DP, Steinbach JP. Loss of cell-matrix contact increases hypoxia-inducible factor-dependent transcriptional activity in glioma cells. Biochem Biophys Res Commun. 2019;515(1):77–84.
26. Du S, Miao J, Zhu Z, Xu E, Shi L, Ai S, Wang F, Kang X, Chen H, Lu X, et al. NADPH oxidase 4 regulates anoikis resistance of gastric cancer cells through the generation of reactive oxygen species and the induction of EGFR. Cell Death Dis. 2018;9(10):948.
27. Liao M, Qin R, Huang W, Zhu HP, Peng F, Han B, Liu B. Targeting regulated cell death (RCD) with small-molecule compounds in triple-negative breast cancer: a revisited perspective from molecular mechanisms to targeted therapies. J Hematol Oncol. 2022;15(1):44.
28. Ashrafizadeh M, Mohammadinejad R, Tavakol S, Ahmadi Z, Roomiani S, Katebi M. Autophagy, anoikis, ferroptosis, necroptosis, and endoplasmic reticulum stress: Potential applications in melanoma therapy. J Cell Physiol. 2019;234(11):19471–9.
29. Barshir R, Fishilevich S, Iny-Stein T, Zelig O, Mazor Y, Guan-Golan Y, Safran M, Lancet D. GeneCaRNA: a comprehensive gene-centric database of human non-coding RNAs in the genecards suite. J Mol Biol. 2021;433(11):166913.
30. Ferreira MR, Santos GA, Biagi CA, Silva Junior WA, Zambuzzi WF. GSVA score reveals molecular signatures from transcriptomes for biomaterials comparison. J Biomed Mater Res A. 2021;109(6):1004–14.
31. Sun D, Wang J, Han Y, Dong X, Ge J, Zheng R, Shi X, Wang B, Li Z, Ren P, et al. TISCH: a comprehensive web resource enabling interactive single-cell transcriptome visualization of tumor microenvironment. Nucleic Acids Res. 2021;49(D1):D1420-d1430.
32. Bakir B, Chiarella AM, Pitarresi JR, Rustgi AK. EMT, MET, plasticity, and tumor metastasis. Trends Cell Biol. 2020;30(10):764–76.
33. Nirmala JG, Lopus M. Cell death mechanisms in eukaryotes. Cell Biol Toxicol. 2020;36(2):145–64.
34. Taddei ML, Giannoni E, Fiaschi T, Chiarugi P. Anoikis: an emerging hallmark in health and diseases. J Pathol. 2012;226(2):380–93.
35. Zhang P, Lv W, Luan Y, Cai W, Min X, Feng Z. Identification and validation of a novel anoikis-related prognostic model for prostate cancer. Mol Genet Genomic Med. 2024;12(4):e2419.

36. Su N, Wang J, Zhang H, Jin H, Miao B, Zhao J, Liu X, Li C, Wang X, Yang N. Identification and clinical validation of the role of anoikis-related genes in diabetic foot. Int Wound J. 2024;21(3):e14771.
37. Guo S, Xing N, Du Q, Luo B, Wang S. Deciphering hepatocellular carcinoma pathogenesis and therapeutics: a study on anoikis, ceRNA regulatory network and traditional Chinese medicine. Front Pharmacol. 2023;14:1325992.
38. Cao L, Zhang S, Peng H, Lin Y, Xi Z, Lin W, Guo J, Wu G, Yu F, Zhang H, et al. Identification and validation of anoikis-related lncRNAs for prognostic significance and immune microenvironment characterization in ovarian cancer. Aging (Albany NY). 2024;16(2):1463–83.
39. Chen YC, Chen CI, Chang CY, Huang BM, Chen YC. Clerodane diterpene induces apoptosis/anoikis and suppresses migration and invasion of human bladder cancer cells through the histone deacetylases, integrin-focal adhesion kinase, and matrix metalloproteinase 9 signalling pathways. Hum Exp Toxicol. 2022;41:9603271221143040.
40. Wang J, Luo Z, Lin L, Sui X, Yu L, Xu C, Zhang R, Zhao Z, Zhu Q, An B, et al. Anoikis-associated lung cancer metastasis: mechanisms and therapies. Cancers (Basel). 2022;14(19):4791.
41. Ge J, Huang Y, Lv M, Zhang C, Talukder M, Li J, Li J. Cadmium induced Fak -mediated anoikis activation in kidney via nuclear receptors (AHR/CAR/PXR)-mediated xenobiotic detoxification pathway. J Inorg Biochem. 2022;227:111682.
42. Sousa B, Pereira J, Marques R, Grilo LF, Pereira SP, Sardão VA, Schmitt F, Oliveira PJ, Paredes J. P-cadherin induces anoikis-resistance of matrix-detached breast cancer cells by promoting pentose phosphate pathway and decreasing oxidative stress. Biochim Biophys Acta Mol Basis Dis. 2020;1866(12):165964.
43. Kim J, Chee WY, Yabuta N, Kajiwara K, Nada S, Okada M. Atg5-mediated autophagy controls apoptosis/anoikis via p53/Rb pathway in naked mole-rat fibroblasts. Biochem Biophys Res Commun. 2020;528(1):146–53.
44. Baghban R, Roshangar L, Jahanban-Esfahlan R, Seidi K, Ebrahimi-Kalan A, Jaymand M, Kolahian S, Javaheri T, Zare P. Tumor microenvironment complexity and therapeutic implications at a glance. Cell Commun Sig. 2020;18(1):59.
45. Erratum: Veenstra RG, Flynn R, Kreymborg K, et al. B7-H3 expression in donor T cells and host cells negatively regulates acute graft-versus-host disease lethality. Blood. 2015;125(21):3335–3346. Blood 2016, 127(24):3104.
46. Maffuid K, Cao Y. Decoding the complexity of immune-cancer cell interactions: empowering the future of cancer immunotherapy. Cancers (Basel). 2023;15(16):4188.
47. Fanfone D, Wu Z, Mammi J, Berthenet K, Neves D, Weber K, Halaburkova A, Virard F, Bunel F, Jamard C, et al. Confined migration promotes cancer metastasis through resistance to anoikis and increased invasiveness. Elife. 2022;11:e73150.
48. Pals ST, Kersten MJ, Spaargaren M. Targeting cell adhesion and homing as strategy to cure Waldenström's macroglobulinemia. Best Pract Res Clin Haematol. 2016;29(2):161–8.
49. Polo-Generelo S, Rodríguez-Mateo C, Torres B, Pintor-Tortolero J, Guerrero-Martínez JA, König J, Vázquez J, Bonzón-Kulichenco E, Padillo-Ruiz J, de la Portilla F, et al. Serpine1 mRNA confers mesenchymal characteristics to the cell and promotes CD8+ T cells exclusion from colon adenocarcinomas. Cell Death Discov. 2024;10(1):116.
50. Escate R, Padro T, Badimon L. LDL accelerates monocyte to macrophage differentiation: effects on adhesion and anoikis. Atherosclerosis. 2016;246:177–86.
51. Di Roio A, Hubert M, Besson L, Bossennec M, Rodriguez C, Grinberg-Bleyer Y, Lalle G, Moudombi L, Schneider R, Degletagne C, et al. Mdr1-expressing Cd4(+) T cells with Th1.17 features resist to neoadjuvant chemotherapy and are associated with breast cancer clinical response. J Immunother Cancer. 2023;11(11):e007733.
52. Turpin R, Liu R, Munne PM, Peura A, Rannikko JH, Philips G, Boeckx B, Salmelin N, Hurskainen E, Suleymanova I, et al. Respiratory complex I regulates dendritic cell maturation in explant model of human tumor immune microenvironment. J Immunother Cancer. 2024;12(4):e008053.
53. Noël G, Fontsa ML, Garaud S, De Silva P, de Wind A, Van den Eynden GG, Salgado R, Boisson A, Locy H, Thomas N, et al. Functional Th1-oriented T follicular helper cells that infiltrate human breast cancer promote effective adaptive immunity. J Clin Invest. 2021;131(19):e139905.
54. Liu L, Zhao WY, Zheng XY. ZNF746 promotes M2 macrophage polarisation and favours tumour progression in breast cancer via the Jagged1/Notch pathway. Cell Signal. 2023;112:110892.
55. Okcu O, Öztürk Ç, Yalçın N, Yalçın AC, Şen B, Aydın E, Öztürk AE. Effect of tumor-infiltrating immune cells (mast cells, neutrophils and lymphocytes) on neoadjuvant chemotherapy response in breast carcinomas. Ann Diagn Pathol. 2024;70:152301.
56. Santana-Hernández S, Suarez-Olmos J, Servitja S, Berenguer-Molins P, Costa-Garcia M, Comerma L, Rea A, Perera-Bel J, Menendez S, Arpí O, et al. NK cell-triggered CCL5/IFNγ-CXCL9/10 axis underlies the clinical efficacy of neoadjuvant anti-HER2 antibodies in breast cancer. J Exp Clin Cancer Res. 2024;43(1):10.
57. Chiocca EA, Yu JS, Lukas RV, Solomon IH, Ligon KL, Nakashima H, Triggs DA, Reardon DA, Wen P, Stopa BM et al: Regulatable interleukin-12 gene therapy in patients with recurrent high-grade glioma: Results of a phase 1 trial. Sci Transl Med. 2019;11(505):eaaw5680.
58. Bangalore Yogananda CG, Shah BR, Vejdani-Jahromi M, Nalawade SS, Murugesan GK, Yu FF, Pinho MC, Wagner BC, Mickey B, Patel TR, et al. A novel fully automated MRI-based deep-learning method for classification of IDH mutation status in brain gliomas. Neuro Oncol. 2020;22(3):402–11.
59. Ye X, Liu Q, Qin X, Ma Y, Sheng Q, Wu X, Chen S, Huang L, Sun Y. BCAR4 facilitates trastuzumab resistance and EMT in breast cancer via sponging miR-665 and interacting with YAP1. Faseb j. 2024;38(7):e23589.
60. Yuan JQ, Xiao Z, Wang SM, Guo L. The prognostic effect of HER2 heterogeneity and YAP1 expression in HER2 positive breast cancer patients: a retrospective study. Gland Surg. 2022;11(2):451–65.
61. Turturro SB, Najor MS, Yung T, Portt L, Malarkey CS, Abukhdeir AM, Cobleigh MA. Somatic loss of PIK3R1 may sensitize breast cancer to inhibitors of the MAPK pathway. Breast Cancer Res Treat. 2019;177(2):325–33.
62. Yan M, Majd MH. Evaluation of Induced apoptosis by biosynthesized zinc oxide nanoparticles in MCF-7 breast cancer cells using Bak1 and Bclx expression. Dokl Biochem Biophys. 2021;500(1):360–7.
63. Bilgic SN, Domaniku A, Toledo B, Agca S, Weber BZC, Arabaci DH, Ozornek Z, Lause P, Thissen JP, Loumaye A, et al. EDA2R-NIK signalling promotes muscle atrophy linked to cancer cachexia. Nature. 2023;617(7962):827–34.
64. Zhu Z, Song J, Guo Y, Huang Z, Chen X, Dang X, Huang Y, Wang Y, Ou W, Yang Y, et al. LAMB3 promotes tumour progression through the AKT-FOXO3/4 axis and is transcriptionally regulated by the BRD2/acetylated ELK4 complex in colorectal cancer. Oncogene. 2020;39(24):4666–80.
65. Ni YH, Zhao X, Wang W. CD24, a review of its role in tumor diagnosis progression and therapy. Curr Gene Ther. 2020;20(2):109–26.
66. Zhu X, Yu J, Ai F, Wang Y, Lv W, Yu G, Cao X, Lin J. CD24 May Serve as an Immunotherapy target in triple-negative breast cancer by regulating the expression of PD-L1. Breast Cancer (Dove Med Press). 2023;15:967–84.
67. Yan S, Wang Y, Chen M, Li G, Fan J. Deregulated SLC2A1 promotes tumor cell proliferation and metastasis in gastric cancer. Int J Mol Sci. 2015;16(7):16144–57.
68. Okcu O, Sen B, Ozturk C, Guvendi GF, Bedir R. GLUT-1 expression in breast cancer. Turk Patoloji Derg. 2022;38(2):114–21.
69. Liao WL, Lin JY, Shieh JC, Yeh HF, Hsieh YH, Cheng YC, Lee HJ, Shen CY, Cheng CW. Induction of G2/M Phase Arrest by Diosgenin via Activation of Chk1 Kinase and Cdc25C Regulatory Pathways to Promote Apoptosis in Human Breast Cancer Cells. Int J Mol Sci. 2019;21(1):172.
70. Althobiti M, El-Sharawy KA, Joseph C, Aleskandarany M, Toss MS, Green AR, Rakha EA. Oestrogen-regulated protein SLC39A6: a biomarker of good prognosis in luminal breast cancer. Breast Cancer Res Treat. 2021;189(3):621–30.

Publisher's Note